INTERNATIONAL JOURNAL OF PRECISION ENGINEERING AND MANUFACTURING Vol. 17, No. 5, pp. 553-564 MAY 2016 / 553
DOI: 10.1007/s12541-016-0068-y ISSN 2234-7593 (Print) / ISSN 2005-4602 (Online)

Two-State GMS-based Friction Model for Precise Control Applications

Fernando Villegas[1,#], Rogelio Lorenzo Hecker[1], and Miguel Peña[2]

1 Facultad de Ingeniería, UNLPam-CONICET, 9 y 110, General Pico, La Pampa, 6360, Argentina
2 Instituto de Automática, UNSJ-CONICET, Av. San Martín 1109(O) San Juan, San Juan, 5400, Argentina
Corresponding Author / E-mail: fvillegas@inaut.unsj.edu.ar, TEL: +54-02302-422780, FAX: +54-02302-422780

KEYWORDS: Friction, Presliding, GMS model, Precise positioning

The capability of a model to represent the complex friction behavior is particularly important for systems where friction has a major impact on motion precision. In this work a GMS-based model is proposed which would require only two states, aiming to simplify the implementation of control laws that require friction models capable of representing presliding friction. Simulations of the proposed model are provided, showing that it keeps the main properties of the GMS model, like hysteresis with nonlocal memory, non-drifting behavior and friction lag. Also, an experimental comparison of the performance of model-based compensation for the proposed two-state model and for the complete GMS model is presented for a linear motor system with linear guides, showing promising results.

Manuscript received: June 27, 2015 / Revised: November 11, 2015 / Accepted: December 14, 2015

NOMENCLATURE

F_f = friction force
x = position
v = velocity
F_i = single GMS element force
ν_i = weight factor associated to the contribution of a single GMS element to net friction force
k_i = single GMS element stiffness
σ_2 = viscous friction coefficient
C = GMS attraction parameter
$s(v)$ = Stribeck curve without viscous term
l_i = transition to slip parameter for element i
t_c = time at which a loop is closed
$t_{s,i}$ = time at which element i starts slipping
Δx = displacement from initial position
${}^k\Delta x$ = displacement from point of motion reversal k
F_s = sticking force
F_d = slipping force
F_γ = correction for varying $s(v)$
F_h = hysteresis and Stribeck contribution to friction force
F_l = friction lag contribution to friction force
$\kappa()$ = nonlinear spring stiffness function
$\Pi()$ = nonlinear spring function
$\gamma()$ = slipping fraction function
φ_i = Deviation of elementary force from $s(v)$ for slipping elements

1. Introduction

Positioning systems subject to external forces under strict precision and speed requirements frequently depend on plain or rolling element bearings for motion guidance. Thus, motion is performed under the effect of friction with a highly non-linear behavior, having a negative impact on motion control performance. Therefore, a suitable model for friction representing most of the observed phenomena is required in order to improve control performance for precision positioning systems.

Static friction models fail to describe all of the phenomena observed in friction, thus, several dynamic models have been proposed. Among the most popular ones is the LuGre model, which captures most of the friction phenomena using a single state dynamic model. However, this model can exhibit drifting behavior under certain conditions[1] and is

unable to reproduce accurately the nonlocal memory characteristics of presliding friction.[2] To overcome these issues, several other models have been proposed, such as the elasto-plastic friction model,[1] the Leuven model[3,4] and the generalized Maxwell-slip (GMS) model.[2,5] In particular, the GMS model accurately represents nonlocal memory, also presenting improvements on friction lag and non-drifting behavior.[2]

The GMS model can accurately represent most of the observed friction behavior. This is a multiple state dynamic model, composed of multiple elements that contribute to the total force. The contribution of individual elements is more apparent during presliding regime. In fact, the curve for presliding hysteresis obtained with this model resembles a piecewise linear function, with as much sections on the total hysteresis curve as model elements. The contribution of each of these elements is updated by integration of a particular dynamic equation, which changes depending on a logic state corresponding to each element. Thus, an accurate representation of presliding hysteresis would require to integrate these switched dynamic equations for a large number of elements, with the respective computational cost implied. Recently, modifications of this model has been proposed to avoid switching dynamics in its elements in order to make it suitable for gradient-based state and parameter estimation, such as in Refs. 6 and 7, yet keeping the same multi-state structure. Instead, the present work seeks to obtain a reduction in the number of states of the friction model, while keeping the description of presliding hysteresis as accurate and smooth as possible.

Hence, this paper presents a two-state model which could describe friction behavior as represented by the GMS model, except for minor deviations due to the simplifications introduced. Section 2 shows a brief recapitulation of the GMS model as described in Ref. 2. That is the same version of the GMS model proposed in Ref. 8 for feedforward compensation and simplified in Ref 9 for adaptive control. Section 3 acts as a motivation to the manner in which the model is approximated and the functions defined therein will be useful in the definition of the proposed model, which is presented in Section 4. Section 5 is devoted to parameter determination. Then, Section 6 shows the behavior of the proposed model by means of simulation, as well as its performance in feedforward compensation in an experimental setup. Finally, the conclusions are presented in Section 7. Also, an appendix is included which expands on some of the results used along the previous sections.

2. GMS Model

The GMS model as described in Ref. 2 can be considered as composed by a parallel arrangement of N single-state dynamic friction elements whose common input is the sliding velocity $v = \dot{x}$, and where each elementary model contributes with a force F_i to the total friction force. The total force for an N-element model results in

$$F_f(t) = \sum_{i=1}^{N} F_i(t) + \sigma_2 v(t) \tag{1}$$

where $\sigma_2 v(t)$ represents viscous friction while the first term accounts for the contribution of all single-state friction elements. A block representation of the model is shown in Fig. 1.

For every elementary model there is a logic state indicating whether the element sticks or slips. If an element sticks, its dynamics is given by

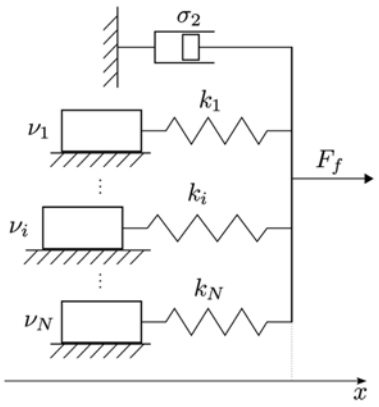

Fig. 1 Representation of the GMS model including viscous friction

$$\frac{dF_i}{dt} = k_i v \tag{2}$$

and the element remains in this condition until $F_i = \nu_i s(v)$. Here k_i is the stiffness of the element and ν_i is a constant related to the contribution of this element to the total force satisfying $0 \le \nu_i \le 1$ and $\Sigma \nu_i = 1$. The function $s(v)$ is such that the friction force for a steady-state velocity v is given by $s(v) + \sigma_2 v$. For instance, a common parametrization of $s(v)$ according to Ref. 2 is

$$s(v) = \mathrm{sgn}(v)\left(F_c + (F_s - F_c)e^{-\left|\frac{v}{V_s}\right|^{\delta_{V_s}}}\right) \tag{3}$$

being F_c the Coulomb force, F_s the static force, V_s the Stribeck velocity and δV_s the Stribeck shape factor.

On the other hand, if the element is slipping, its dynamics is given by

$$\frac{dF_i}{dt} = \mathrm{sgn}(v)\nu_i C\left(1 - \frac{F_i}{\nu_i s(v)}\right) \tag{4}$$

where C is called the attraction parameter and the elementary model keeps slipping until the velocity crosses zero.

Before proposing a two-state simplified model for friction, the next section attempts to rearrange the GMS model equations as a motivation for the proposed model.

3. Rearrangement of the GMS Model Equations

Each element of the GMS model have a sticking and a slipping regime, contributing during both regimes to the net force arising from friction elements. In the remaining section, a distinction is considered between the part of the net elementary force contributed by elements during all of its sticking regime, which is discussed in Section 3.1, and that contributed by those elements during slipping regime, considered in Section 3.2.

Thus, the GMS equations corresponding to the individual elements are rearranged in order to combine the original states of all these el-

ements in a few new states. In sections 3.1 and 3.2 this is done exclusively for a motion beginning from a particular state until reaching again zero velocity. Then, in Section 3.3 the results are extended to the whole motion trajectory although allowing some deviations from the GMS model.

3.1 Sticking force for motion from zero state

In a general case, considering an initial condition $F_{i,0} = F_i(t_0)$ the force contributed by element i at time t while sticking (see Eq. (2)) can be expressed as

$$F_i(t) = F_{i,0} + \int_{t_0}^{t} k_i v(\tau) d\tau = F_{i,0} + k_i(x(t) - x_0) \tag{5}$$

where $x(t)$ represents the common position input, $x_0 = x(t_0)$, and the element remains sticking until $F_i(t) = v_i s(v)$.

To begin with the rearrangement, it is considered an initial state for the elements such that $F_{i,0} = 0$ for $i = 1, \ldots, N$ with all elements sticking, which will be further called zero state. Then, as a first step the sticking force is obtained for a movement starting from zero state. Thus, the force resulting from the elements during sticking regime is initially

$$F_s(t) = \sum_{i=1}^{N} F_i(t) = \sum_{i=1}^{N} \int_{t_0}^{t} k_i v(\tau) d\tau = \int_{t_0}^{t} \sum_{i=1}^{N} k_i v(\tau) d\tau \tag{6}$$

being this the sticking force and also the net elementary force. Eq. (6) holds until the first element begins slipping. Considering Eq. (5) the condition for transition to slip of element i, i.e., $F_i = v_i s(v)$, during the initial motion can be written as

$$x(t) - x_0 = \frac{v_i}{k_i} s(v(t)) \tag{7}$$

Then, an element i starts slipping at a time $t_{s,i}$ when

$$\frac{x(t_{s,i}) - x_0}{s(v(t_{s,i}))} = l_i \tag{8}$$

where $l_i = v_i/k_i$. Without loss of generality it can be considered that the elements are ordered in a descending order of l_i, that is $i < j \Leftrightarrow l_i > l_j$. Such an ordering would mean that the first elements to start slipping would be the last ones (first the element N, then N–1 and so on), because the velocity input is common to all elements.

Now, every time an element starts slipping, it will cease to contribute to the sticking force. Considering this, the total sticking force from t_0 to the point of motion reversal can be expressed in a more general and compact manner as

$$F_s = \int_{t_0}^{t} \sum_{i=1}^{N} k_i \left(1 - h\left(\frac{\Delta x(\tau)}{s(v(\tau))} - l_i\right)\right) v d\tau \tag{9}$$

where $\Delta x(\tau) = x(\tau) - x(t_0)$ and $h(\xi)$ is the Heaviside function, defined as

$$h(\xi) = \begin{cases} 0, & \xi < 0 \\ 1, & \xi \geq 0 \end{cases} \tag{10}$$

Then, defining $\kappa_0(\xi)$ as

$$\kappa_0(\xi) = \sum_{i=1}^{N} k_i (1 - h(\xi - l_i)) \tag{11}$$

the sticking force can be written as

$$F_s(t) = \int_{t_0}^{t} \kappa_0\left(\frac{\Delta x(\tau)}{s(v(\tau))}\right) v d\tau \tag{12}$$

In this way, the contribution to the sticking force of all the N elements at an arbitrary time t during motion from zero state is expressed in a compact form.

3.2 Slip contribution for motion from zero state

When considering slipping elements, it can be seen from Eq. (4) that when element i slips, the solution $F_i(t)$ must hold the following integral equation:

$$F_i(t) = F_i(t_{s,i}) + \int_{t_{s,i}}^{t} \operatorname{sgn}(v(\tau)) C\left(v_i - \frac{F_i(\tau)}{s(v(\tau))}\right) d\tau \tag{13}$$

where $F_i(t_{s,i})$ is the element force when the element begins slipping, at time $t_{s,i}$.

For an individual element i, the quantity $\Delta F_i = F_i(t) - F_i(t_{s,i})$ can be expressed in a more convenient manner extending the lower limit of the integral, expressing the slipping condition by means of the Heaviside function:

$$\begin{aligned} \Delta F_i &= \int_{t_{s,i}}^{t} \operatorname{sgn}(v(\tau)) C\left(v_i - \frac{F_i(\tau)}{s(v(\tau))}\right) d\tau \\ &= -\int_{t_0}^{t} \frac{1}{|s(v(\tau))|} C F_i(\tau) h\left(\frac{\Delta x(\tau)}{s(v(\tau))} - l_i\right) d\tau \\ &\quad + \int_{t_0}^{t} \frac{1}{|s(v(\tau))|} C v_i s(v(\tau)) h\left(\frac{\Delta x(\tau)}{s(v(\tau))} - l_i\right) d\tau \end{aligned} \tag{14}$$

However, recalling that $F_i(t_{s,i})$ corresponds to the end of the sticking regime for element i, such that $F_i(t_{s,i}) = v_i s(v(t_{s,i}))$, the same quantity can be expressed, for continuous acceleration, as

$$\begin{aligned} \Delta F_i &= F_i(t) - v_i s(v(t)) + v_i s(v(t)) - v_i s(v(t_{s,i})) \\ &= (F_i(t) - v_i s(v(t))) + \int_{t_{s,i}}^{t} v_i \frac{ds \circ v}{dt} d\tau \\ &= (F_i(t) - v_i s(v(t))) + \int_{t_0}^{t} v_i h\left(\frac{\Delta x(\tau)}{s(v(\tau))} - l_i\right) \frac{ds \circ v}{dt} d\tau \end{aligned} \tag{15}$$

Here $s \circ v(t) = s(v(t))$ and it is assumed that $s(v)$ is differentiable for $v \in (-\infty, 0) \cup (0, \infty)$ and both $\lim_{v \to 0^+} s(v)$ and $\lim_{v \to 0^-} s(v)$ exist.

The last subsection considered the contribution of elements in sticking regime to the total force. In this subsection the effect of the elements during slipping regime on the total force is considered. Such a contribution will be represented by the term F_d. Initially, when all elements stick, $F_d = 0$. Thereafter, for each slipping element, a term $F_i(t) - F_i(t_{s,i})$ is added to F_d. Considering the transition to slip of the different elements along the displacement, this quantity can be expressed as $F_d = \Sigma_{i=1}^{N} (F_i(t) - F_i(t_{s,i})) h\left(\frac{\Delta x(\tau)}{s(v(\tau))} - l_i\right)$. Considering Eqs. (14) and (15), and proceeding as done for the net sticking force, a relation for F_d can be obtained, based on the following quantity involving all slipping elements:

$$F_l = \sum_{i=1}^{N} (F_i(t) - v_i s(v(t))) h\left(\frac{\Delta x(t)}{s(v(t))} - l_i\right) \tag{16}$$

resulting that

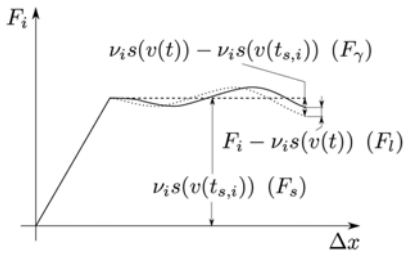

Fig. 2 Contribution of an individual element to F_s, F_l, F_γ

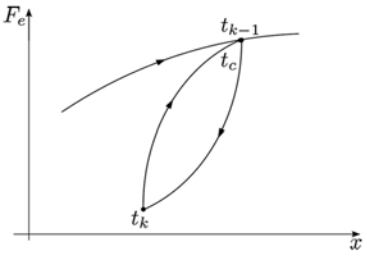

Fig. 3 Inner loops

$$F_l = -\int_{t_0}^{t} \left[\frac{1}{|s(v(\tau))|} CF_l + \gamma_0\left(\frac{\Delta x(\tau)}{s(v(\tau))}\right) \frac{ds \circ v}{dt} \right] d\tau \tag{17}$$

where

$$\gamma_0(\xi) = \sum_{i=1}^{N} v_i h(\xi - l_i) \tag{18}$$

And this quantity allows to calculate F_d as $F_d = F_l + F_\gamma$ where

$$F_\gamma = \int_{t_0}^{t} \gamma_0\left(\frac{\Delta x(\tau)}{s(v(\tau))}\right) \frac{ds \circ v}{dt} d\tau \tag{19}$$

According to Eq. (16), F_l can be regarded as the deviation of the total force of the slipping elements from that corresponding solely by the Stribeck curve, due to its dynamic behavior dictated by Eq. (13). As such, at the beginning, when all elements stick, such a quantity would be zero, and Eq. (17) can be considered as a relation of the type used to describe the slipping dynamics in Eq. (13).

Thus, the net elementary force can be obtained as $F = F_s + F_l + F_\gamma$, where F_γ is related to the difference in the value of the Stribeck curve between the current time and the time when the respective elements started slipping. A convenient way to visualize these quantities is considering that each of F_s, F_l and F_γ results from the contribution of individual elements during its motion. For instance, Fig. 2 shows a graphical representation of the contribution of element i to each of these quantities for a slipping element along its displacement.

It should be noticed that F_s and F_γ can be combined in a single state $F_h = F_s + F_\gamma$, in which case its dynamics will be given by

$$F_h = \int_{t_0}^{t} \left[\kappa_0\left(\frac{\Delta x(\tau)}{s(v(\tau))}\right) v(\tau) + \gamma_0\left(\frac{\Delta x(\tau)}{s(v(\tau))}\right) \frac{ds^{\circ} v}{dt} \right] d\tau \tag{20}$$

As previously stated, this is valid for a motion starting from zero state as long as zero velocity is not reached. In that event, if velocity reaches zero at t_{zv}, all the elements change to stick state, $F_l(t_{zv}^+) = F_\gamma(t_{zv}^+) = 0$ and the net force becomes the force of sticking elements resulting $F_h(t_{zv}^+) = F_h(t_{zv}^-) + F_l(t_{zv}^-)$ being this the initial condition for the next motion. Here, the notation $f(t_1^+)$ and $f(t_1^-)$ stand for $\lim_{t \to t_1^+} f(t)$ and $\lim_{t \to t_1^-} f(t)$ respectively.

Before proposing a model based on this rearrangement, it must be considered the manner in which the defined quantities vary for different initial conditions.

3.3 Extension to the whole motion trajectory

It is still necessary to consider the manner in which the results for motion from zero state can be extended to the whole motion trajectory. In this section a short overview is given, but more detail can be found in sections A.3 and A.4 of the appendix. It should be noticed that these rules correspond only approximately to the GMS model, as an exact representation would require a significant increase in the complexity of the proposed model. More information about the simplifications introduced can be found in the aforementioned sections.

As a first step it should be considered the dynamics of the elements sticking after reaching zero velocity (initially all of them). The situation is quite similar to the one for motion from zero state, except for the initial state of all elements, which will affect the point of transition to slip of the different elements. When the body reaches zero velocity and then continues motion in the same direction, the previously slipping elements can be considered to continue slipping. In such a case the transition of the sticking elements afterward is given by the same functions κ_0 and γ_0 and the states do not change at that point.

In the case of motion reversal, approximately the same equations can be used except that the arguments of functions $\kappa_0(\xi)$ and $\gamma_0(\xi)$ are given by $\xi = {}^k\Delta x(t)/(s(v(t)) - s(v(t_k^-)))$, being ${}^k\Delta x(t) = x(t) - x(t_k)$ and $x(t_k)$ the last point of motion reversal. Here the points of motion reversal are indexed as $k = 0, 1, 2, \ldots$ corresponding $k = 0$ to zero state. This argument is used until a new motion reversal, until loop closure or until return to the virgin curve, i.e., the friction-displacement curve described during motion from zero state, which would happen when $k = 1$ and

$$\frac{{}^1\Delta x(t)}{s(v(t)) - s(v(t_1^-))} = \frac{\Delta x(t_1)}{s(v(t_1^-))} \tag{21}$$

In the latter case, the last point $x(t_k)$ to consider is again $x(t_0)$, $k = 0$ and the arguments of κ_0 and γ_0 are once again given by $\Delta x(t)/s(v(t))$.

A similar case occurs in the event of a loop closure, when after two consecutive motion reversals the elements slipping immediately before the last motion reversal t_k^- are again slipping (see Fig. 3) and elements slipping at t_{k-1}^- begin to slip again. In this case, for the model proposed in Section 4 it is considered that elements slipping for the last time at t_{k-1}^- begin to slip at the same instant t_c, when

$$\frac{{}^k\Delta x(t_c)}{s(v(t_c)) - s(v(t_k^-))} = \frac{{}^{k-1}\Delta x(t_k)}{s(v(t_k^-)) - s(v(t_{k-1}^-))} \tag{22}$$

To correct at some extent this simplification, the states are updated at time t_c as

$$F_h(t_c^+) = F_h(t_{k-2}) + \Pi(\beta_c)(s(v(t_c)) - s(v(t_{k-2}^-))) \tag{23}$$

where

$$\beta_c = \frac{{}^{k-2}\Delta x(t_c)}{s(v(t_c)) - s(v(t_{k-2}^-))} \tag{24}$$

and $\Pi(\xi)$ is a primitive of a nonlinear spring stiffness function such that $\Pi(0) = 0$. More details about these functions can be seen in Section 4 where the proposed model is presented.

From then on, the argument to use in functions κ_0 and γ_0 after loop closure is ${}^{k-2}\Delta x/(s(v(t)) - s(v(t_{k-2}^-)))$ when $k > 2$ or $\Delta x/s(v(t))$ when k=2.

Although these results may suggest the necessity to keep the previous values of $s(v(t))$ at times of motion reversal, this is not exactly the case. As acceleration was presumed to be continuous, the value $s(v(t_k^-))$ corresponds to $\lim_{v\to 0+} s(v)$ or $\lim_{v\to 0-} s(v)$ depending on the motion direction previous to the point of motion reversal. To simplify the exposition, it will be assumed here that $s(v)$ has odd symmetry, although it is not difficult to adapt the model to other case. Also, the quantity s_{st} is defined as $s_{st} = \lim_{v\to 0+} s(v) = -\lim_{v\to 0-} s(v)$. Then, for continuous acceleration, if t_k corresponds to the last point of motion reversal (or more precisely to the instant at which zero velocity is reached before motion reversal) then $s(v(t_k^-)) = -\mathrm{sgn}(v)s_{st}$.

Finally, it should be pointed out that the loop closure conditions must be considered only when there are elements sticking at t_k^-, as such conditions correspond to the transition to slip of these elements after the last point of motion reversal. Thus, if $x(t_k^-)$ is beyond the presliding region, there are no elements sticking at that point and the loop closure condition is not considered. In such a case this point of motion reversal is kept as the reference of the arguments in the equations and previous points of motion reversal are no longer considered for motion in the same direction. The point $x(t_k^-)$ will be inside the presliding region when

$$\frac{{}^{k-1}\Delta x(t_k)}{s(v(t_k^-)) - s(v(t_{k-1}^-))} \le l_1 \tag{25}$$

A similar situation occurs with the return to the virgin curve, except that the condition to be considered is

$$\frac{\Delta x(t_1)}{s(v(t_1^-))} \le l_1 \tag{26}$$

In the same manner, when this condition does not hold, condition in Eq. (21) will not be considered and $x(t_1)$ will be kept as the reference in the arguments of the equation.

4. Proposed Model

Based on the previous sections, an approximate model will be proposed where $\kappa_0(\xi)$ and $\gamma_0(\xi)$ are replaced by continuous functions $\kappa(\xi)$ and $\gamma(\xi)$ as shown in Fig. 4, which allows to represent such functions with just a few parameters. In order to make this approximation, functions κ and γ are required to satisfy several properties corresponding to those of κ_0 and γ_0 and shown in more detail in Section A.1 of the appendix.

Then, the proposed model can be expressed as follows. Friction dynamics is given by the following 2-state system (obtained from derivation of Eqs. (20) and (17))

$$\begin{aligned}\frac{dF_h}{dt} &= \kappa\left(\frac{{}^k\Delta x(t)}{s(v(t)) - s_k}\right)v(t) + \gamma\left(\frac{{}^k\Delta x(t)}{s(v(t)) - s_k}\right)\frac{ds\circ v}{dt}\\ \frac{dF_l}{dt} &= -\frac{C}{|s(v(t))|}F_l - \gamma\left(\frac{{}^k\Delta x(t)}{s(v(t)) - s_k}\right)\frac{ds\circ v}{dt}\end{aligned} \tag{27}$$

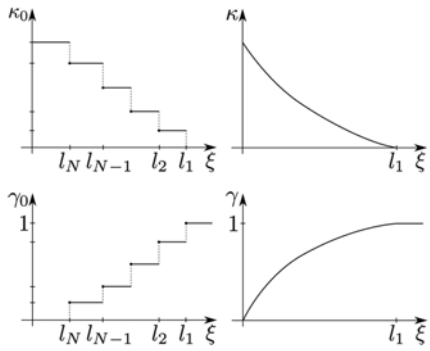

Fig. 4 κ and γ in the proposed model in contrast with κ_0 and γ_0

where k is the index of the last motion reversal to be considered, ${}^k\Delta x(t) = x(t) - x(t_k)$ and the net friction force is still given by $F = F_h + F_l + \sigma_2 v$. For motion from zero state, it is considered that $s_0 = 0$. Instead, for $k \ge 1$ the value $s_k = s(v(t_k^-)) = -\mathrm{sgn}(s(v(t))) \cdot s_{st}$, thus the quantity $s(v(t)) - s_k$ is approximately $2s(v(t))$. For the first motion ($k = 0$), $x(t_0)$ is the initial position and if the system begins from zero state then $F_h = F_l = 0$. The model requires to keep two stacks of values, one with points of motion reversal and the other with the respective values of F_h. The arguments on the equations change after each motion reversal or loop closure according to the following rules:

Rule 1 If motion direction changes at x_d, k is incremented by 1, and both $x(t_k) = x_d$ and $F_h(t_k^-)$ are saved to the stacks. Then, the states are updated as $F_l(t_k^+) = 0$ and $F_h(t_k^+) = F_h(t_k^-)$.

Although there is a deviation from the GMS in not adding $F_l(t_k^-)$ to F_h as seen in Section 3.2, it is necessary because of having neglected the deviation of elementary force from $s(v)$ for slipping elements, φ_i, when the argument for motion reversal was determined (see Section A.3 of the appendix). This is required to obtain the force corresponding by the Stribeck curve for stationary velocity.

Rule 2 When a loop is closed, that is when

$${}^k\Delta x(t) = -({}^{k-1}\Delta x(t_k))\frac{|s(v(t))| + s_{st}}{2s_{st}} \tag{28}$$

and the following condition holds:

$$\frac{|{}^{k-1}\Delta x(t_k)|}{2s_{st}} \le l_1 \tag{29}$$

the states are updated as

$$\begin{aligned}F_h(t_c^+) &= F_h(t_{k-2}) + \Pi(\beta_c)(s(v(t_c)) - s(v(t_{k-2}^-)))\\ F_l(t_c^+) &= F_l(t_c^-)\end{aligned} \tag{30}$$

where β_c is given by Eq. (24). Then k is reduced by 2, and the last 2 elements of each stack are removed. As previously described, Π is a function related to the nonlinear spring stiffness function κ and is defined as $\Pi(\xi) = \int_0^\xi \kappa(u)du$.

Rule 3 (Only when the system begins from zero state) When $k = 1$, $|{}^1\Delta x(t)| = \frac{|s(v(t))| + s_{st}}{s_{st}}|\Delta x(t_1)|$ and $|\Delta x(t_1)|/s_{st} \le l_1$, k returns to 0, the last element of each stack is removed, and the states remain unchanged in the transition point.

It is worth to mention that in addition to the points removed from

stack because of loop closure, there will be more elements of the stack which can be removed due to the conditions regarding l_1 in rules 2 and 3. This will allow to reduce in some degree the amount of memory required in the implementation of this algorithm.

Finally, it should be noticed that the evolution of the state F_h between points of discontinuity can also be obtained without the need of integration as shown in Section A.2. In fact, if t_d is the last point of state discontinuity, where the state is updated to the value $F_h(t_d^+)$, and the arguments of κ and γ in Eq. (27) are referenced to the point of motion reversal at $x(t_k)$, then

$$F_h(t) = F_h(t_d^+) + \left[\Pi\left(\frac{{}^k\Delta x}{s(v) - s_k} \right) (s(v) - s_k) \right]_{t_d}^{t} \tag{31}$$

which reduces to

$$F_h(t) = F_h(t_k^+) + \Pi\left(\frac{{}^k\Delta x(t)}{s(v(t)) - s_k} \right) (s(v(t)) - s_k) \tag{32}$$

when $t_d = t_k$. In this manner, F_h can be constructed by a set of rules in a manner resembling Masing rules for hysteresis.[10] This allows to update one of the states without performing any numerical integration, which is needed only for the state related to friction lag. Furthermore, a simplified model without friction lag can be obtained considering just the state F_h and thus not requiring any integration.

5. Parameter Determination

The procedure for obtaining the Stribeck curve parameters would consist as usual on performing constant velocity motions, for which force is given by $F = s(v) + \sigma_2 v$, as shown in Section A.2 of the appendix, and fitting the data for different velocities to a parameterization of $s(v)+\sigma_2 v$.

As for determination of $\kappa(x)$ it can be obtained by performing constant speed motions at equal low velocity along the presliding region, for instance following a saw-tooth reference position. In such a case, if relative position from a point of motion reversal is given by $x = v_s t$, then friction force (or its variation from the value at $x = 0$) is dependent on the position from the point of motion reversal, that is $F = F(x)$, and $\frac{dF}{dt} = \frac{dF}{dx} v_s$. Hence, if $\frac{ds \circ v}{dt}$ can be neglected

$$\frac{dF}{dx} = \kappa\left(\frac{x}{2s(v_s)} \right) \tag{33}$$

Thus, one manner would be fitting a curve to $F(x)$ on this experiment and deriving the analytic expression, in order to obtain κ from Eq. (33), for which it would only be needed a scale change to obtain $\kappa(\xi)$. Then, Π can be calculated as $\Pi(\xi) = \int_0^{\xi} \kappa(u) du$, and considering the properties of κ and γ, in particular (A-3), $\gamma(\xi)$ can be obtained as $\gamma(\xi) = \Pi(\xi) - \xi\kappa(\xi)$. It should be noticed that due to the properties of $\kappa()$, the parameterization of $F(x)$ should be constant for $x > 2s(v_s)l_1$. Thus, considering a piecewise-defined function, the process would imply the fitting of a curve to $F(x)$ for $x \le 2s(v_s)l_1$.

As for the attraction parameter C, one way is to perform a varying positive velocity motion as suggested for the GMS model in Ref. 2. As C is the only unknown parameter, F_l is obtained as $F_l = F - F_h - \sigma_2 v$, from which dF_l / dt is calculated and C is obtained fitting the data to the proposed model equations (Eq. (27)).

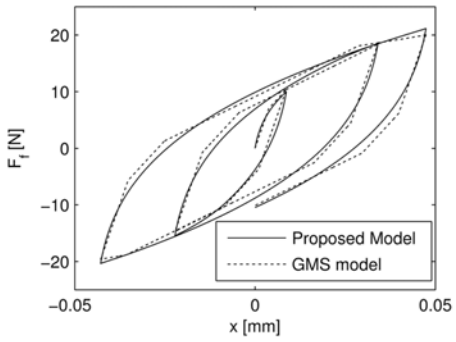

Fig. 5 Comparison of GMS and proposed model under simulation for presliding regime

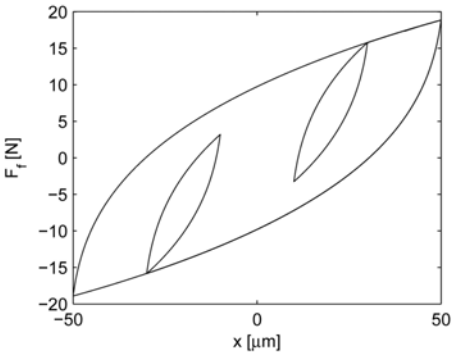

Fig. 6 Presliding friction for the proposed model

6. Results

In this section, simulation and experimental results are shown for the proposed model. First, simulation results show the behavior of the proposed model in a variety of friction conditions. Then, experimental results are shown for feedforward compensation performance of the proposed model in comparison with that of the GMS model.

6.1 Simulation results

A simulation of the proposed model and a 5-element GMS model for motions in the presliding regime is shown in Fig. 5. There, the proposed model presents a continuous slope change along each branch of the hysteresis loop in contrast to the abrupt slope changes for the GMS model. This is an advantage of the proposed model as is shown further in the experimental results.

Also, simulation of the proposed model in presliding regime for a different input is shown in Fig. 6, where it can be seen that when a loop is closed, the main loop is followed again. This is the expected behavior of hysteresis with nonlocal memory, one of the known properties[2] of presliding friction.

A property verified in the model for the sliding regime is the friction lag. In Fig. 7, a positive velocity with a periodical component is applied to the friction model, which results in a hysteresis loop around the Stribeck curve, as shown in Ref. 11.

Another important property of friction is the non-drifting behavior.[2]

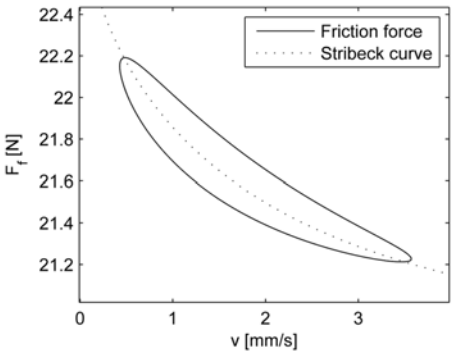

Fig. 7 Friction lag as represented by the proposed model

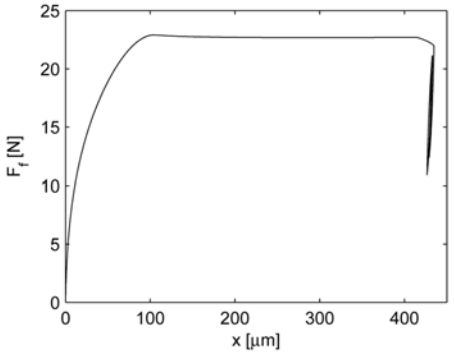

Fig. 8 Non-drifting behavior of the proposed model

To verify whether a model is capable of exhibiting this behavior a particular time-varying force[1] must be applied to a mass with the proposed friction model. In the simulation the first part of the applied force is a ramp which reaches a value higher than that of breakaway force, falling immediately to a value below Coulomb friction. Then the applied force oscillates around this value without reaching the breakaway force. The result for the proposed model is shown in Fig. 8, where it can be seen the non-drifting behavior, as the mass position oscillates around the same point during the oscillatory part of the force.

6.2 Experimental results

The performance of the proposed model for feedforward control has been tested on the linear motor stage shown in Fig. 9. Here the friction force comes from the four ball runner blocks with 8% of preload, sliding over linear guides. The linear drive is based on a permanent magnet linear synchronous motor. Position measurement is performed with a high resolution linear scale. More details about the particular system can be found in Ref. 12.

The system is controlled by a pole-placement state-space controller with integral action and model based feedforward. A diagram of the whole control structure is shown in Fig. 10. The state-space controller with full state observer as well as the inclusion of integral action follows the typical structure shown in Ref. 13. The observer has a deadbeat design and the controller poles are at $z_1 = 0.9624$, $z_{2,3} = 0.9617 \pm j0.0376$. Also, a zero phase error tracking controller was set following the procedure in Ref. 14, having one uncancellable closed-loop zero at $z =$

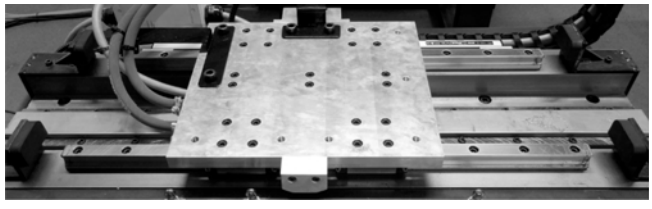

Fig. 9 Linear motor stage

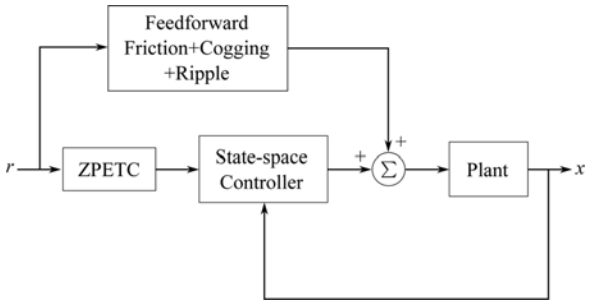

Fig. 10 Control diagram for the experiment

48.5807. The feedforward signal considers cogging and ripple as modeled in Ref. 12, as well as model based friction compensation. Being just a feedforward signal it will not affect closed loop stability.

The performance of the proposed model for feedforward compensation has been compared to that of two other models, the simple Tustin model and the GMS model. The Tustin model for friction is solely based on the Stribeck curve, as is described in Ref. 15 where this model is used for control design. A 5-element GMS model is also considered, as its number of states is comparable to that of the proposed model. Also, in order to perceive the importance of the reduction of slope changes in presliding, a 10-element GMS model is set.

The parameters for Tustin model are those corresponding to the Stribeck curve, which are shown in Table 1, and the procedure followed for obtaining them is described in Ref. 12. The GMS models also have the attraction parameter, which is C = 10.8 N/s and the hysteresis parameters, which are shown in Table 2 for the 5-element model and in Table 3 for the 10-element model. These parameters had also been determined following the procedure in Ref. 12. For the proposed model, instead of presliding parameters there are interrelated functions which can be obtained from a parameterization for $F(x)$ in the interval $[0, 2s(v_s)l_1]$ as described in Sec. 5. In the particular experiments carried on in this work the chosen parameterization is $F(x) = K - ae^{b(x+\beta)^{\alpha}} - cx^4$ where $K = ae^{b\beta^{\alpha}}$ for the parameters a = 2631 N, b = –0.0438 mm$^{-0.3}$, c = 2367.9 N/mm^4, α = 0.3, β = 1×10^{-3} mm and l_1 = 0.004 291 mm/N.

First, the system is commanded to follow a 5 mm amplitude sinusoidal reference with a 6 s period. Fig. 11 shows the position error for the friction models tested. It can be seen that the maximum error for Tustin based feedforward reaches 75.2 μm, being 13 μm for the 5-element GMS model, 11.5 μm for the 10-element GMS model and 9.8 μm for the proposed model. Thus, for this motion amplitude the performance obtained in feedforward control with the proposed model is better than that of the GMS model while requiring the update of just

Table 1 Stribeck curve parameters

F_s [N]	F_c [N]	V_s [mm/s]	δV_s	σ_2 [Ns/mm]
26.1	21.6	3.1	0.6	0.054

Table 2 Hysteresis parameters for 5-element GMS model

v_i	0.17	0.13	0.30	0.017	0.38
k_i [N/mm]	1152.07	377.23	215.33	9.39	87.66

Table 3 Hysteresis parameters for 10-element GMS model

v_i	0.1198	0.0077	0.0809	0.0841	0.0053
k_i [N/mm]	2051.68	47.15	288.57	248.35	10.37
v_i	0.0505	0.139	0.0895	0.0355	0.3876
k_i [N/mm]	60.05	104.15	58.05	19.99	92.16

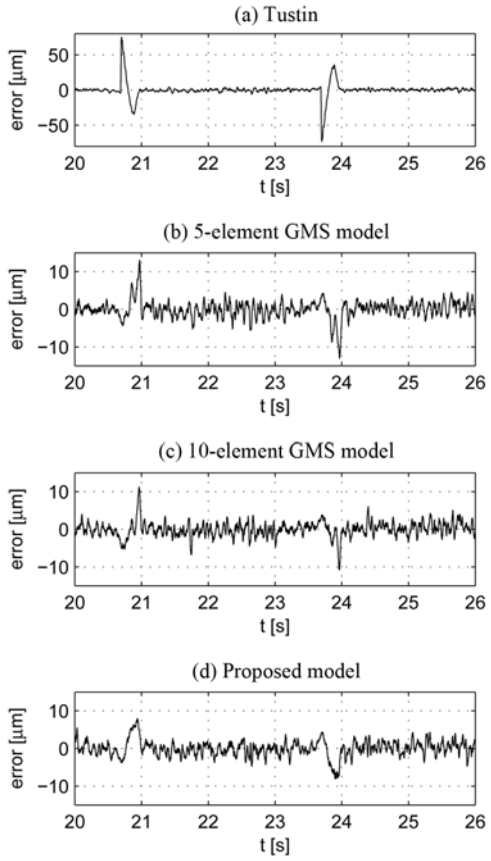

Fig. 11 Comparison of model performance in feedforward control for 5 mm amplitude sinusoidal reference

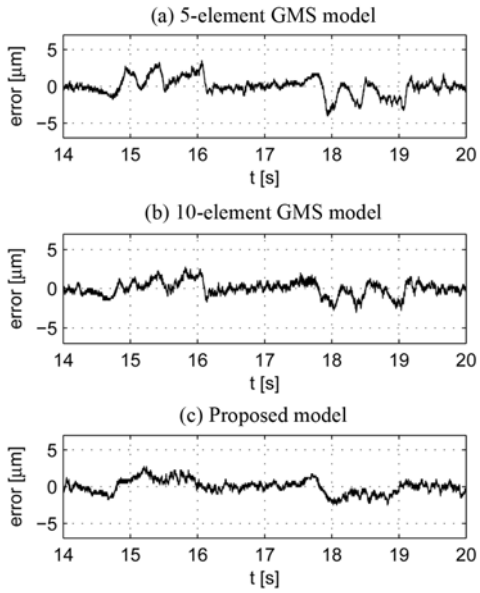

Fig. 12 Comparison of model performance in feedforward control for 250 μm amplitude sinusoidal reference

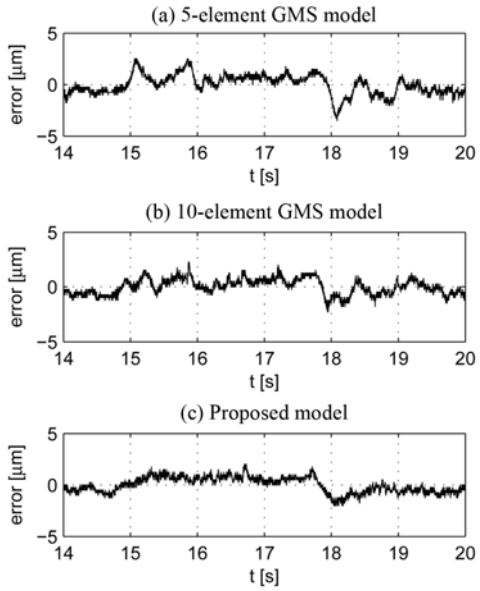

Fig. 13 Comparison of model performance in feedforward control for 100 μm amplitude sinusoidal reference

two states. Besides, it is clear that the performance of both, the GMS and the proposed model, far exceeds the Tustin model, which is no longer considered in the following tests.

Fig. 11 also shows the peaks of maximum error, which occur at motion reversal, where friction is in presliding regime. In order to fully study the error behavior in the presliding regime, a set of experiments has been performed with smaller motion amplitudes as follow: 250 μm in Fig. 12, 100 μm in Fig. 13 and 50 μm in Fig. 14. The first observation in these experiments is the oscillatory behavior of the error clearly seen when the 5-element GMS model is used for compensation, and in a minor degree for the 10-element model, in contrast to the proposed model. This seems to be a result of the integral control reacting to the discontinuities of the slope changes reflected in the feedforward term, which were pointed out in Fig. 5. As a consequence, the maximum error in each experiment for the proposed model is lower respect to the GMS model. The maximum errors for both models are summarized in Table 4 for the purpose of comparison.

The previous experiments have been repeated for the proposed model and the 5-element GMS, adding a 15.5 kg load to the motor to test the robustness of this compensation strategy for different conditions. The results are shown in Table 5, where it can be seen that the errors are very

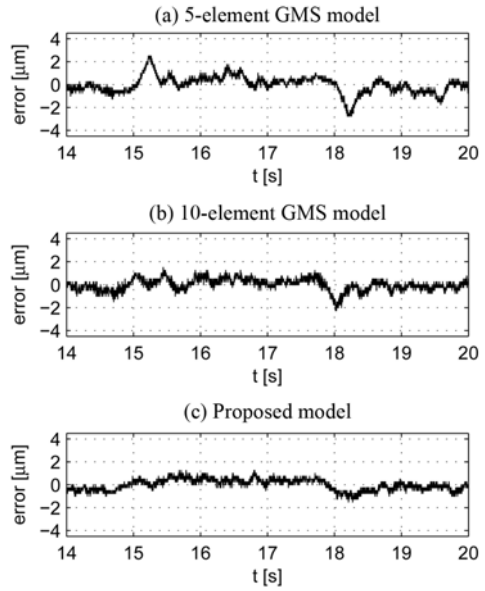

Fig. 14 Comparison of model performance in feedforward control for 50 μm amplitude sinusoidal reference

Table 4 Maximum position error for motor without additional load

Amplitude	5 mm	250 μm	100 μm	50 μm
Proposed model	9.8 μm	3 μm	2.2 μm	1.5 μm
10-element GMS model	11.5 μm	3.2 μm	2.5 μm	2.5 μm
5-element GMS model	13 μm	4.3 μm	3.7 μm	3 μm

Table 5 Maximum position error for motor with additional load

Amplitude	5 mm	250 μm	100 μm	50 μm
Proposed model	11.8 μm	3.5 μm	3.2 μm	2 μm
5-element GMS model	15.3 μm	3.7 μm	3.7 μm	3 μm

similar to those obtained without load (see Table 4). In fact the maximum error for the proposed model is still lower to that of the 5-element GMS in this case.

7. Conclusion

The present work shows a two-state model based on the GMS model, keeping the main model properties including friction lag, Stribeck effect, presliding friction and non-drifting behavior.

Its performance for feedforward compensation has been tested for several references, where the error obtained was lower to that of the GMS model, mainly due to its performance on presliding regime. This improvement is attributed to the continuity of slope change inside the hysteresis loop exhibited by the proposed model, in contrast to the GMS model. Additional tests were performed with an extra load obtaining similar results to the experiments without load.

Furthermore, the proposed model only requires the update of two states which is convenient for real time implementation on certain systems. Moreover, the definition of these states allows obtaining one of them without performing any integration, leaving only one state to integrate in order to consider the effect of friction lag.

ACKNOWLEDGEMENT

The authors would like to thank CONICET, ANPCyT and UNLPam for the financial support of this work through the projects CONICET PIP 00531 and ANPCyT-UNLPam PICTO2011-0263.

REFERENCES

1. Dupont, P., Armstrong, B., and Hayward, V., "Elasto-Plastic Friction Model: Contact Compliance and Stiction," Proc. of the American Control Conference, pp. 1072-1077, 2000.
2. Lampaert, V., "Modelling and Control of Dry Sliding Friction in Mechanical Systems," Ph.D. Thesis, Department of Mechanical Engineering, Katholieke Universiteit Leuven, 2003.
3. Swevers, J., Al-Bender, F., Ganseman, C. G., and Projogo, T., "An Integrated Friction Model Structure with Improved Presliding Behavior for Accurate Friction Compensation," IEEE Transactions on Automatic Control, Vol. 45, No. 4, pp. 675-686, 2000.
4. Lampaert, V., Swevers, J., and Al-Bender, F., "Modification of the Leuven Integrated Friction Model Structure," IEEE Transactions on Automatic Control, Vol. 47, No. 4, pp. 683-687, 2002.
5. Al-Bender, F., Lampaert, V., and Swevers, J., "The Generalized Maxwell-Slip Model: A Novel Model for Friction Simulation and Compensation," IEEE Transactions on Automatic Control, Vol. 50, No. 11, pp. 1883-1887, 2005.
6. Boegli, M., De Laet, T., De Schutter, J., and Swevers, J., "A Smoothed GMS Friction Model Suited for Gradient-based Friction State and Parameter Estimation," IEEE/ASME Transactions on Mechatronics, Vol. 19, No. 5, pp. 1593-1602, 2014.
7. Boegli, M., De Laet, T., De Schutter, J., and Swevers, J., "Moving Horizon for Friction State and Parameter Estimation," Proc. of European Control Conference (ECC), pp. 4142-4147, 2013.
8. Jamaludin, Z., "Disturbance Compensation for Machine Tools with Linear Motor Drives," Ph.D. Thesis, Department of Mechanical Engineering, Katholieke Universiteit Leuven, 2008.
9. Nilkhamhang, I. and Sano, A., "Adaptive Compensation of a Linearly-Parameterized GMS Friction Model with Parameter Projection," Proc. of 45th IEEE Conference on Decision and Control, pp. 6271-6276, 2006.
10. Al-Bender, F., Symens, W., Swevers, J., and Van Brussel, H., "Theoretical Analysis of the Dynamic Behavior of Hysteresis Elements in Mechanical Systems," International Journal of Non-Linear Mechanics, Vol. 39, No. 10, pp. 1721-1735, 2004.
11. Al-Bender, F. and De Moerlooze, K., "Characterization and Modeling of Friction and Wear: An Overview," Sustainable Construction and Design, Vol. 2, No. 1, pp. 19, 2011.
12. Villegas, F., Hecker, R., Peña, M., Vicente, D., and Flores, G., "Modeling of a Linear Motor Feed Drive including Pre-Rolling

Friction and Aperiodic Cogging and Ripple," The International Journal of Advanced Manufacturing Technology, Vol. 73, No. 1, pp. 267-277, 2014.

13. Franklin, G. F., Powell, J. D., and Workman, M. L., "Digital Control of Dynamic Systems," Addison-Wesley, 1998.

14. Tomizuka, M., "Zero Phase Error Tracking Algorithm for Digital Control," Journal of Dynamic Systems, Measurement, and Control, Vol. 109, No. 1, pp. 65-68, 1987.

15. Tan, K. K., Lee, T. H., and Huang, S., "Precision Motion Control: Design and Implementation," Springer, 2008.

APPENDIX

A.1 Properties of κ and γ

Functions κ_0 and γ_0 are defined motivated on Eqs. (11) and (18). From such equations, functions should have the shape shown on Fig. 15.

Function κ_0 is positive, decreasing and has unitary area as can be seen on Fig. 16, as $k_i l_i = \nu_i$ and $\Sigma_{i=1}^{N} \nu_i = 1$.

An important property involving both functions can be seen when integrating $\kappa_0(\xi)$ from a point of transition l_m:

$$\begin{aligned}\int_{l_m}^{l_1} \kappa_0(u)du &= \sum_{i=1}^{m-1} k_i(l_{m-1}-l_m)+\sum_{i=1}^{m-2} k_i(l_{m-2}-l_{m-1})+\ldots+k_1(l_1-l_2)\\ &= k_1(l_1-l_m)+k_2(l_2-l_m)+\ldots+k_{m-1}(l_{m-1}-l_m)\\ &= \sum_{i=1}^{m-1} k_i l_i - l_m\sum_{i=1}^{m-1} k_i = \sum_{i=1}^{N} k_i l_i - \sum_{i=m}^{N} k_i l_i - l_m\sum_{i=1}^{m-1} k_i\\ &= \sum_{i=1}^{N} \nu_i - \sum_{i=m}^{N} \nu_i - l_m\sum_{i=1}^{m-1} k_i = 1-\gamma_0(l_m)-l_m\kappa_0(l_m)\end{aligned} \tag{A-1}$$

This property holds for any number of elements for integration from transition points. As the number of element increases, the distance between transition points diminishes accordingly.

In the proposed model, κ_0 and γ_0 are replaced by continuous functions κ and γ, which allow to represent such functions with just a few parameters. As in κ_0 and γ_0, for $\xi \geq l_1$ holds $\kappa(\xi) = 0$ and $\gamma(\xi) = 1$. Also, as if each point of the interval [0 l_1] would be a transition point, it will be considered that both functions fulfill the same properties stated before, that is

$$\int_0^{l_1} \kappa(u)du = 1 \tag{A-2a}$$

$$\int_\xi^{l_1} \kappa(u)du = 1-\gamma(\xi)-\xi\kappa(\xi) \tag{A-2b}$$

The last property will allow to obtain $\gamma(\xi)$ once $\kappa(\xi)$ is known. Also, the last property can be rearranged based on the first one and considering that $\int_0^{l_1} \kappa(u)du = \int_0^{\xi} \kappa(u)du + \int_\xi^{l_1} \kappa(u)du$. Then, the following expression can be obtained:

$$\int_0^{\xi} \kappa(u)du = \gamma(\xi)+\xi\kappa(\xi) \tag{A-3}$$

which can also be used to obtain $\gamma(\xi)$ from $\kappa(\xi)$.

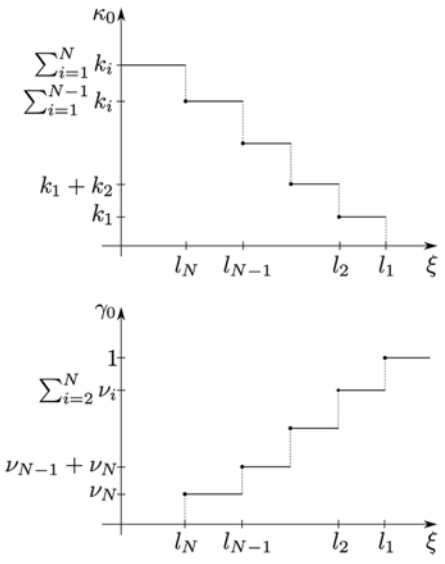

Fig. 15 κ_0 and γ_0

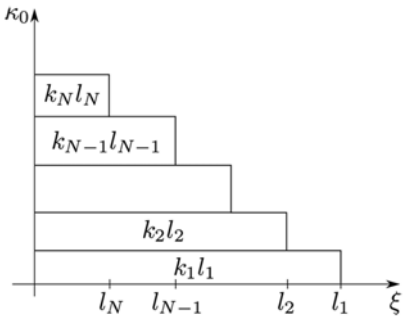

Fig. 16 Area for κ_0

A.2 Friction force for stationary speed

For simplicity it will be considered the case where no intermediate state updates are performed, that is when no loop closure nor return to virgin curve occurs. Let t_1 be the time for the beginning of a new displacement after motion reversal, and t_l the time at which presliding region is surpassed during this displacement, that is when ${}^1\Delta x(t_l)/(s(v(t_l)) - s_1) = l_1$. From Eq. (27), F_h at t_l is given by

$$\begin{aligned}F_h(t_l) = F_h(t_1)&+\int_{t_1}^{t_l} \kappa\left(\frac{{}^1\Delta x(\tau)}{s(v(\tau))-s_1}\right)v(\tau)d\tau\\ &+\int_{t_1}^{t_l} \gamma\left(\frac{{}^1\Delta x(\tau)}{s(v(\tau))-s_1}\right)\frac{ds\circ v}{dt}(\tau)d\tau\end{aligned} \tag{A-4}$$

From properties in Section A.1, $\gamma\left(\frac{{}^1\Delta x}{s(v)-s_1}\right)$ can be expressed as

$$\gamma\left(\frac{{}^1\Delta x}{s(v)-s_1}\right) = \Pi\left(\frac{{}^1\Delta x}{s(v)-s_1}\right)-\frac{{}^1\Delta x}{s(v)-s_1}\kappa\left(\frac{{}^1\Delta x}{s(v)-s_1}\right) \tag{A-5}$$

where

$$\Pi\left(\frac{{}^1\Delta x}{s(v)-s_1}\right) = \int_0^{\frac{{}^1\Delta x}{s(v)-s_1}} \kappa(u)du \tag{A-6}$$

Then, (A-4) can be put as

$$F_h(t_l) = F_h(t_1) + \int_{t_1}^{t_l} \Pi\left(\frac{{}^1\Delta x}{s(v)-s_1}\right)\frac{ds^\circ v}{dt}d\tau + \int_{t_1}^{t_l} \kappa\left(\frac{{}^1\Delta x}{s(v)-s_1}\right)\left[v - \frac{{}^1\Delta x\frac{ds^\circ v}{dt}}{s(v)-s_1}\right]d\tau \quad \text{(A-7)}$$

Integrating by parts, the first integral can be written as

$$\Gamma = \int_{t_1}^{t_l} \Pi\left(\frac{{}^1\Delta x}{s(v)-s_1}\right)\frac{ds^\circ v}{dt}d\tau = \left[\Pi\left(\frac{{}^1\Delta x}{s(v)-s_1}\right)(s(v)-s_1)\right]_{t_1}^{t_l} - \int_{t_1}^{t_l} \kappa\left(\frac{{}^1\Delta x}{s(v)-s_1}\right)\left[v - \frac{{}^1\Delta x\frac{ds^\circ v}{dt}}{s(v)-s_1}\right]d\tau \quad \text{(A-8)}$$

In such a manner, (A-4) is reduced to

$$F_h(t_l) = F_h(t_1) + \left[\Pi\left(\frac{{}^1\Delta x}{s(v)-s_1}\right)(s(v)-s_1)\right]_{t_1}^{t_l} \quad \text{(A-9)}$$

As t_l is the instant when the presliding region is surpassed, $\Pi\left(\frac{{}^1\Delta x(t_l)}{s(v(t_l))-s_1}\right) = 1$. On the other hand, at the beginning of the displacement $\Pi\left(\frac{{}^1\Delta x(t_1)}{s(v(t_1))-s_1}\right) = 0$. Thus

$$F_h(t_l) = F_h(t_1) + s(v(t_l)) - s_1 \quad \text{(A-10)}$$

A similar result can be obtained for a displacement from zero state, except that s_1 would be replaced by $s_0 = 0$. Then, if the displacement before motion reversal started from zero state, and considering rule 1 from Section 4, $F_h(t_1) = s_1$. Thus, F_h at time t_l results $F_h(t_l) = s(v(t_l))$. Once surpassed the presliding region, $\kappa\left(\frac{{}^1\Delta x(t)}{s(v(t))-s_1}\right) = 0$, $\gamma\left(\frac{{}^1\Delta x(t)}{s(v(t))-s_1}\right) = 1$ and the only effect on F_h by the proposed model is to add $s(v(t)) - s(v(t_l))$. Hence, outside the presliding region $F_h(t) = s(v(t))$.

If a new motion reversal occurs, the same procedure can be followed to show that after the presliding regime $F_h(t) = s(v(t))$ once again.

Regarding the complete friction force, after reaching a stationary velocity v_s, $ds^\circ v / dt = 0$. Then, as C is positive and $s(v_s)$ is bounded, it can be shown that $F_l \to 0$, and $F \approx F_h + \sigma_2 v$. In such a case $F \approx s(v_s) + \sigma_2 v_s$.

It should also be noticed from the previous discussion that the same procedure can be applied to obtain the evolution of F_h between points of state discontinuity. For instance, if t_d is the last point of state discontinuity, where the state is updated to the value $F_h(t_d^+)$, and the arguments of κ and γ in Eq. (27) are referenced to the point of motion reversal at $x(t_k)$, then

$$F_h(t) = F_h(t_d^+) + \left[\Pi\left(\frac{{}^k\Delta x}{s(v)-s_k}\right)(s(v)-s_k)\right]_{t_d}^{t} \quad \text{(A-11)}$$

A.3 Motion reversals

For motion from zero state, the slipping transition was reflected in the arguments of functions $\kappa_0(\xi)$ and $\gamma_0(\xi)$, through terms of the form $h(\xi - l_i)$. Such a term account for the transition to slip of an element i whenever the argument $\xi = l_i$. For a motion from zero state the argument was $\xi = \Delta x(t)/s(v(t))$. However, for the following motions, instead of beginning from an initial condition of zero force as in Eq. (6), every element has an initial force which may differ from zero. The effect of this initial force will be to modify the arguments of κ_0 and γ_0 until the next time zero velocity is reached.

Suppose there has been k motion reversals, where the last motion reversal occurred at t_k. Now, proceeding as done to obtain Eq. (7) but considering that $F_{i,0} = F_i(t_k) \neq 0$ in Eq. (5), the elements will be sticking while

$$-v_i|s(v(t))| - F_i(t_k) \le k_i \cdot {}^k\Delta x(t) \le v_i|s(v(t))| - F_i(t_k) \quad \text{(A-12)}$$

where $F_i(t_k)$ is the initial condition of that element after motion reversal, being t_k the time at which the object reached zero velocity. Suppose element i was slipping until that point. As already known, the force while slipping is being attracted to the curve $v_i s(v)$.[2] For convenience this force at time t_k, $F_i(t_k)$, will be written as

$$\begin{aligned} F_i(t_k) &= v_i s(v(t_k^-)) + (F_i(t_k) - v_i s(v(t_k^-))) \\ &= v_i s(v(t_k^-)) + v_i \varphi_i(t_k^-) \end{aligned} \quad \text{(A-13)}$$

where

$$\varphi_i(t_k^-) = \frac{F_i(t_k) - v_i s(v(t_k^-))}{v_i} \quad \text{(A-14)}$$

Then, the sticking condition in (A-12) can be expressed as

$$-l_i|s(v(t))| - l_i s(v(t_k^-)) - l_i\varphi_i(t_k^-) \le {}^k\Delta x(t)$$
$${}^k\Delta x(t) \le l_i|s(v(t))| - l_i s(v(t_k^-)) - l_i\varphi_i(t_k^-)$$

where depending on the sign of velocity, ${}^k\Delta x(t)$ will increase or decrease defining one particular condition for transition to slip. Then, for a motion reversal, where $s(v(t))$ and $s(v(t_k^-))$ have opposite sign, the sticking condition can be put in a more convenient manner as

$$\frac{{}^k\Delta x(t)}{s(v(t)) - s(v(t_k^-))} \le l_i - l_i\frac{\varphi_i(t_k^-)}{s(v(t)) - s(v(t_k^-))} \quad \text{(A-15)}$$

The term $\varphi_i(t_k^-)/(s(v(t)) - s(v(t_k^-)))$ is related to the deviation from the Stribeck curve due to friction lag. The excursions from the Stribeck curve are expected to be smaller when the attraction parameter is bigger, or when the variation of $s(v)$ for velocities in the same direction are smaller. If $\varphi_i(t_k^-)/(s(v(t)) - s(v(t_k^-)))$ can be neglected, which amounts to neglect the effect of friction lag on the force position relation during presliding regime, the slipping condition can be expressed as

$$\frac{{}^k\Delta x(t)}{s(v(t)) - s(v(t_k^-))} \le l_i \quad \text{(A-16)}$$

Thus, while the elements that begin to slip are those previously slipping, the arguments of κ_0 and γ_0 would be given by the left side of (A-16).

Here it was described the case of a motion reversal. In the same manner, it can be shown that when the body reaches zero velocity and then continues motion in the same direction, the slipping elements can be considered to continue slipping. In such a case the transition of the sticking elements afterward will be given by the same functions κ_0 and γ_0 and the states do not change at that point.

This section primarily showed the situation of slipping elements after motion reversal. However, it still needs to be described the situation of the elements sticking immediately before motion reversal. Consider the particular case when $k = 1$. After motion reversal at t_1 the arguments are

those previously shown, which account for the elements previously slipping at t_1^-. However, regarding the elements not slipping at t_1^-, as the force of each element at t_1 is given by $F_i(t_1) = k_i\Delta x(t_1)$, its force after motion reversal is $F_i(t) = k_i \cdot \Delta x(t)$ until the element slips. Then, the slipping condition for these elements corresponds again to Eq. (8), and the arguments of κ_0 and γ_0 are once again given by $\Delta x(t)/s(v(t))$ once these elements begin to slip.

To obtain the point where these elements start to slip, it is convenient to consider that for the first motion the slipping condition Eq. (8) does not hold for these elements. Hence, the l_i of these elements is such that $l_i \gtrapprox \Delta x(t_1)/s(v(t_1^-))$. Thus, after the first motion reversal, considering (A-16), these elements will begin to slip when

$$\frac{{}^1\Delta x(t)}{s(v(t))-s(v(t_1^-))} \approx \frac{\Delta x(t_1)}{s(v(t_1^-))} \tag{A-17}$$

A similar case arises when considering the closure of inner loops, described in Section A.4.

A.4 Loop closure

It can be shown that the first elements to slip since t_k (see Fig. 3) will be those with the smaller values of l_i, which are already slipping at t_k^-. Also, the next elements to slip will be those with the next bigger values of l_i, which were slipping for the last time at t_{k-1}.

In this section, the condition for elements sticking at t_k^- to begin slipping is considered. This condition will be referred to as the condition for loop closure. Conversely, a motion will be considered part of an inner loop if the set of slipping elements is a subset of those elements slipping before the last motion reversal. Then, after t_k those elements will not slip while the following condition holds:

$$\left|k_i {}^{k-1}\Delta x(t) + v_i s(v(t_{k-1}^-)) + v_i\varphi_i(t_{k-1}^-)\right| \le v_i\left|s(v(t))\right| \tag{A-18}$$

In order to simplify, here is considered only the case for positive velocity at time t, although similar conclusions can be drawn for the other case. Proceeding as before, (A-18) leads to the condition

$${}^{k-1}\Delta x(t) \le l_i(s(v(t)) - s(v(t_{k-1}^-)) - \varphi_i(t_{k-1}^-)) \tag{A-19}$$

As velocity at times t and t_{k-1}^- have the same direction, the right side of the inequality might be close to zero. In such a case the elements slipping for the last time at t_{k-1}^- will begin to slip over a small region in the nearings of ${}^{k-1}\Delta x(t) = 0$. Although this transition could be accounted for as done for the transition to slip shown in previous section, this might result in practical problems when implemented in an approximate model.

To avoid the aforementioned problems in the proposed model, it is considered that these elements begin to slip at the same instant t_c. In order to make such a simplification however, the state F_h should be corrected to account for the transition to slip of these elements, and for the integration of κ and γ along values which would still correspond to some of these elements in stick state. A correction term can be obtained considering (A-11) along a complete loop. Thus, defining the instant t_c of transition to slip as

$$\frac{{}^k\Delta x(t_c)}{s(v(t_c))-s(v(t_k^-))} = \frac{{}^{k-1}\Delta x(t_k)}{s(v(t_k^-))-s(v(t_{k-1}^-))} \tag{A-20}$$

the correction term amounts to a compensation of the speed difference between instants t_c and t_{k-1}^-, resulting

$$F_h(t_c^+) = F_h(t_{k-2}) + \Pi(\beta_c)(s(v(t_c)) - s(v(t_{k-2}^-))) \tag{A-21}$$

where

$$\beta_c = \frac{{}^{k-2}\Delta x(t_c)}{s(v(t_c))-s(v(t_{k-2}^-))} \tag{A-22}$$

Regarding F_l, the elements which begin to slip over this small region start with zero deviation from the Stribeck curve, so it will be assumed that the net deviation can be neglected. In this maner, F_l will stay as previously to loop closure.

From there on the elements which will begin to slip are those which were sticking at t_{k-1} and that were slipping for the last time at t_{k-2}. Considering the slipping condition for these elements, as done in (A-18) for elements slipping in t_{k-1}, it can be seen that the argument to use in functions κ and γ after loop closure ${}^{k-2}\Delta x/(s(v(t)) - s(v(t_{k-2}^-)))$.

Although the previous treatment was for a generic point of motion reversal at an inner loop, the same applies when $k - 2 = 0$, that is when loop closure occurs at the first motion reversal, except that the elements that will begin to slip are those which has never slip, resulting that the argument after loop closure will now be $\Delta x/s(v(t))$.